The 5th Joint International Conference on Multibody System Dynamics
June 24 – 28, 2018, Lisboa, Portugal

The Shimmy Phenomenon in Dynamics of Driven Rigid Castor Wheel

Alexandra A. Zobova[1]

[1] *Department of Mechanics and Mathematics, Lomonosov Moscow State University, azobova@mech.math.msu.su*

ABSTRACT — *Shimmy (or wobble) is a phenomenon of quick oscillation of a steerable wheel of a vehicle. We study the dynamics of a castor wheel driven by a constant force. The wheel touches the horizontal plane: depending on the contact model the dynamics of the system differs significantly. We explore three models: ideal non-holonomic constraint, dissipative non-holonomic constraint and dry friction in the contact patch between the wheel and the plane. The third model is a model of a deformable rough plane: we assume that Coulomb friction is distributed on the non-zero contact patch between the wheel and the plane. For this model we study the stability of the steady rectilinear motion of the wheel: it is shown that for some critical value of the wheel's speed a Poincaré-Andronov-Hopf bifurcation occurs.*

1 Introduction

The dynamics of the systems with friction is of great interest as friction appears in all non-ideal contacts between the surfaces. The investigation of friction has very long history: it includes the experimental studies and models' construction, application of the models in particular mechanical systems, building of effective analytical and numerical method for the analysis [1]. Shimmy is a phenomenon of quick bar angle oscillation that friction induces in a steerable wheel of light aircraft or other vehicles. It occurs when the rectilinear motion of the wheel in a fork loses its stability through Poincaré-Andronov-Hopf bifurcation as it was shown for the simplest model of pneumatic tires in [2], see also [3]. The proper pneumatic tires modelling is complicated due to the continuum medium involved, and the methods for its accurate numerical simulation are illustrated by the system with shimmy phenomenon [4]. However, the complexity of the system makes the stability analysis of the system hard to perform. Quite simple model with only 3 degree of freedom with classic Coulomb friction (in a stiction and sliding regimes) was investigated in [5], [6], and the qualitative results including the analysis of the chaos appearing after Poincaré-Andronov-Hopf bifurcation are impressive (notice, that in this model the suspension is equipped with a spring). Besides, the existence of shimmy was shown also in the case of so-called polycomponent dry friction [7]: this model takes into account non-zero area of the contact patch and, consequently, the decreasing of the dry friction force due to the spinning.

In this article, we study the dynamics of the castor absolutely rigid wheel in rigid fork that is driven by a constant force along a rough horizontal plane (the statement of the problem is in the Sect. 2). We compare three models: ideal non-holonomic constraint (Sect. 3), dissipative non-holonomic constraint (Sect. 4) and dry friction in the contact patch between the wheel and the plane (Sect. 5). It is assumed that non-slipping is provided by Coulomb dry friction force in the stiction regime: we analyze whether the reaction lies inside the friction cone. In the third model (distributed dry friction [8]) due to the differential form of Coulomb dry friction and dynamic distribution of normal stresses in the contact patch the friction force and torque depend both on slipping velocity and angular velocity of the wheel. The linear stability analysis for the third model is given in Sect. 5.2, 5.3.

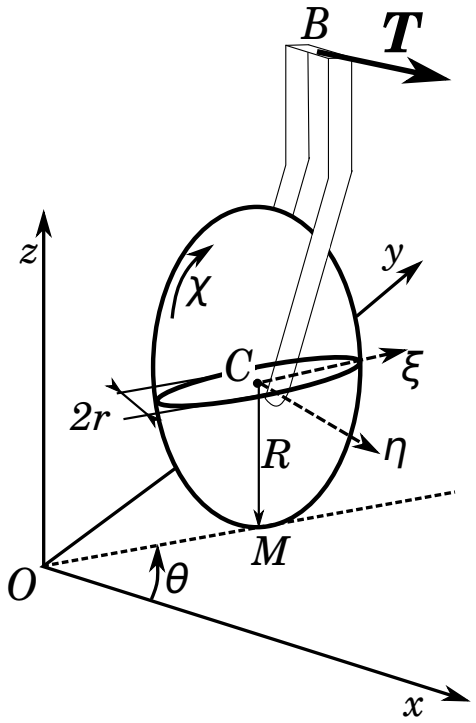

Fig. 1: Driven castor wheel: the notations

2 The Statement of the Problem

We consider the motion of an absolutely rigid wheel of mass m and radius R along a fixed horizontal plane Oxy (Fig. 1). The wheel is mounted in a weightless fork so that it rotates smoothly about its principal axis $C\eta$. We introduce a moving frame $C\xi\eta z$ attached to the fork: the origin is in the wheel's center C, the coordinate plane $C\xi z$ is the middle plane of the wheel. A driving force $\boldsymbol{T} = T\boldsymbol{e}_x$ (with constant value and direction, $T > 0$) is applied to the point B of the fork. Its radius-vector is $\boldsymbol{CB} = b\boldsymbol{e}_\xi + h\boldsymbol{e}_z$, so the offset of the castor-wheel equals b. The middle plane of the wheel stays vertical. We denote the lowest point of the wheel by M, so that $\boldsymbol{CM} = -R\boldsymbol{e}_z$: the point M is the contact point in case of point contact and belongs to the contact patch in case of extended contact.

We use the following coordinates: x, y, z are the absolute coordinates of the center C, course angle θ is the angle between Ox and $C\xi$, and χ is the proper angle of the wheel's rotation. Besides, we denote by v_ξ, v_η, v_z the projections of the wheel center's velocity onto the axes $C\xi$, $C\eta$ and Cz respectively; J_1, J_3 are the inertia moments with respect to Cz and $C\eta$.

We consider three models of wheel-plane interaction: nonholonomic constraint that expresses the absence of sliding (ideal and dissipative cases) and rolling with sliding along the rough plane with dry friction in the contact area. To get the equations of motion for both models in a similar way, we denote the friction force or the component of reactions by $\boldsymbol{F} = F_\xi\boldsymbol{e}_\xi + F_\eta\boldsymbol{e}_\eta + F_z\boldsymbol{e}_z$ and dry friction torque with respect to the point M by $\boldsymbol{M} = M_\xi\boldsymbol{e}_\xi + M_\eta\boldsymbol{e}_\eta + M_z\boldsymbol{e}_z$. Let $\boldsymbol{R} = R_\xi\boldsymbol{e}_\xi + R_\eta\boldsymbol{e}_\eta + R_z\boldsymbol{e}_z$ be the resultant reaction which provide the connection between the fork and the wheel and $\boldsymbol{L} = L_\xi\boldsymbol{e}_\xi + L_\eta\boldsymbol{e}_\eta + L_z\boldsymbol{e}_z$ be the reaction torque with respect to the point C. We assume that the cylinder joint between the fork and the wheel being ideal, so we have $L_\eta = 0$.

The equations of motion are

$$\begin{aligned}
\dot{z} &= v_z && (1)\\
m\dot{v}_z &= F_z - mg + R_z && (2)\\
m(\dot{v}_\xi - v_\eta\dot{\theta}) &= F_\xi + R_\xi && (3)\\
m(\dot{v}_\eta + v_\xi\dot{\theta}) &= F_\eta + R_\eta && (4)\\
0 &= -R_z && (5)\\
0 &= -R_\xi + T\cos\theta && (6)\\
0 &= -R_\eta - T\sin\theta && (7)\\
J_1\ddot{\theta} &= M_z + L_z && (8)\\
J_3\ddot{\chi} &= -F_\xi R + M_\eta && (9)\\
0 &= -L_z - bT\sin\theta && (10)
\end{aligned}$$

Here Eqs. (2)–(4) and Eqs. (5)–(7) express the momentum theorem projected onto the moving frame $C\xi\eta z$ for the wheel and the fork respectively. Eqs. (8)–(9) and (10) express the angular momentum theorem with respect to the mass center for the wheel (projections on $C\eta$ and Cz axis) and for the fork (on Cz axis).

Excluding the reactions in the fork-wheel joint, we get:

$$\begin{aligned}
\dot{z} &= v_z && (11)\\
m\dot{v}_z &= F_z - mg && (12)\\
m(\dot{v}_\xi - v_\eta\dot{\theta}) &= F_\xi + T\cos\theta && (13)\\
m(\dot{v}_\eta + v_\xi\dot{\theta}) &= F_\eta - T\sin\theta && (14)\\
J_1\ddot{\theta} &= M_z - bT\sin\theta && (15)\\
J_3\ddot{\chi} &= -F_\xi R + M_\eta && (16)
\end{aligned}$$

To close this system, we need to define how F_ξ, F_η, F_z M_η, M_z depend on phase variables. We do it and study the dynamics in the following sections.

3 Ideal differential constraint

Here we consider the case of the absolutely rigid wheel moving along the plane without sliding. So following constraints are imposed on the system

$$v_\xi - R\dot{\chi} = 0,\ v_\eta = 0,\ v_z = 0 \tag{17}$$

In addition we assume here that the constraints are ideal, thus we have

$$M_\eta = 0,\ M_z = 0 \tag{18}$$

After differentiating and excluding the reactions from (11)–(16), we get the following closed ODE system:

$$\begin{aligned}
J_1\ddot{\theta} + bT\sin\theta &= 0 && (19)\\
(J_3 + mR^2)\ddot{\chi} &= TR\cos\theta && (20)
\end{aligned}$$

and the reactions are

$$F_z = mg,\ F_\xi = -jT\cos\theta,\ F_\eta = T\sin\theta + mR\dot{\chi}\dot{\theta}, \text{where } j = \frac{J_3}{J_3 + mR^2} \le \frac{1}{2} \tag{21}$$

In [9], it was shown how to derive the dynamic equations Eqs. (19-20) in laconic way without reactions' introducing.

Eq. (19) has the form of pendulum equation and separates from Eq. (20). So, there exists the motions $\theta = 0,\ \pi$ with arbitrary speed of the center $v_\xi(t) = R\dot{\chi}(t)$. The motion $\theta \equiv 0$ are stable with respect to the variable θ and this property does not depend on the speed V_ξ: on the motions in the vicinity of $\theta = 0$, the wheel accelerates since $\ddot{\chi} > 0$ for $\theta \in (-\pi/2, \pi/2)$ according to Eq. (20). On these motions, the center of mass follows the point B of the force T application. On the contrary, the motions $\theta \equiv \pi$ are unstable w.r.t. θ — in this case, the wheel rotates about the vertical axis.

However, Eqs. (19-20) govern the dynamics of the wheel only when the constraint of non-slipping (18) is hold. To check this, we assume that dry Coulomb friction force assures non-slipping. Then the reaction $\boldsymbol{F}$ should be inside the friction cone defined by inequality

$$\sqrt{F_\xi^2 + F_\eta^2} \le f F_z \tag{22}$$

where f is a friction coefficient.

We study the projection of the region, where Ineq. (22) holds, on the $(\theta, \dot{\theta})$-plane (we call it FC-region). On the motions $\theta \equiv 0,\ \pi$, the reaction is aligned with the wheel $|F_\xi| = jT$, $F_\eta = 0$, and Ineq. (22) is fulfilled when $T \le j^{-1}mg$. In this case, the FC-region contain some motions in the neighbourhood of the motion $\theta \equiv 0$ for small $\dot{\chi}$. Indeed, the squared Ineq. (22) takes the form:

$$T^2(\sin^2\theta + j^2\cos^2\theta) + 2mTR\sin\theta\dot{\chi}\dot{\theta} + m^2R^2\dot{\chi}^2\dot{\theta}^2 \le f^2m^2g^2$$

The intersection of the FC-region with the axis $\dot{\theta} = 0$ can be found from

$$T^2(1 + (j^2-1)\cos^2\theta) \le f^2m^2g^2 \Longrightarrow \cos^2\theta \ge \frac{1 - T^{-2}f^2m^2g^2}{1 - j^2}$$

The last inequality has non-empty solution if $T \le j^{-1}fmg$. The FC-regions on a phase portrait of Eq. 19 for different value of T are shown on Fig. 2.

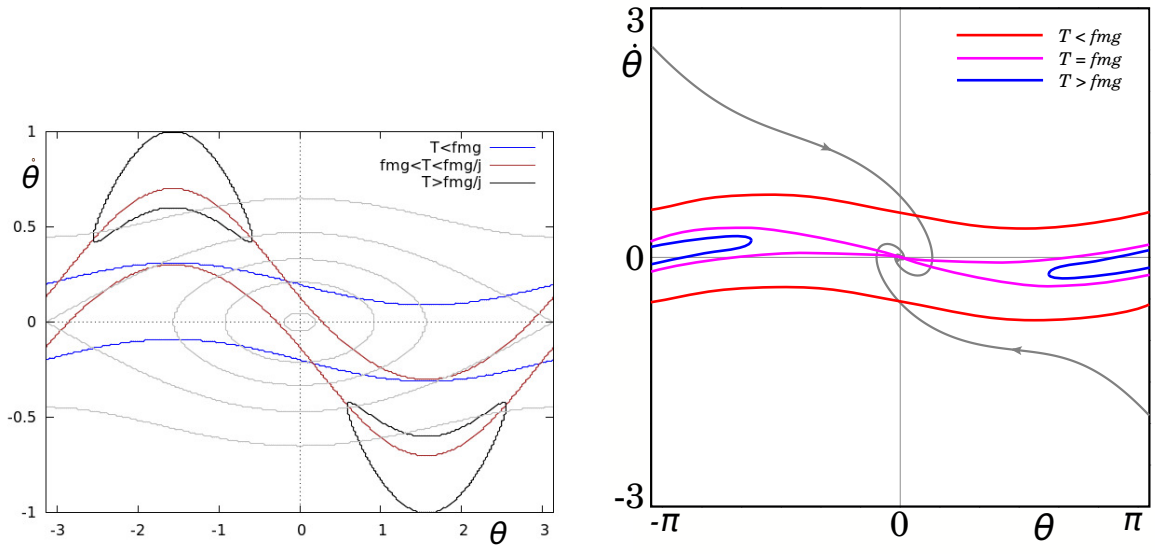

Fig. 2: Phase portrait and the regions where the reaction lies in a friction cone. On the left panel: ideal case, the FC-regions collapse to the abscissa-axis while $\dot{\chi} \to +\infty$. On the right: dissipative case, FC-regions are plotted for maximal velocity $\dot{\chi} = TR/c_1$

However, since Ineq. 3 depends on the product $\dot{\theta}\dot{\chi}$, FC-region tightens to the x-axis when $\dot{\chi}$ increases. This means that at some instant slipping occurs on any arbitrary small oscillation $\theta(t)$ in the vicinity of rectilinear

motion $\theta \equiv 0$. It means that this motion can loose stability when the wheel begins to slip. In the next section, we show that adding dissipation in the system with differential contraint Eq. (18) permits to have stable rectilinear motion without slipping.

4 Dissipative differential constraint

Now we add rolling and spinning friction of viscous type:

$$M_\eta = -c_1\dot{\chi},\ M_z = -c_2\dot{\theta}, \quad c_1 > 0,\ c_2 > 0 \tag{23}$$

Then Eqs. (19, 20) take the form:

$$J_1\ddot{\theta} + bT\sin\theta = -c_2\dot{\theta} \tag{24}$$

$$(J_3 + mR^2)\ddot{\chi} = TR\cos\theta - c_1\dot{\chi} \tag{25}$$

The solution $\theta = 0$ becomes asymptotically stable, and the wheel's proper angular velocity is bounded:

$$\dot{\chi} = \frac{TR}{c_1} + \left(\dot{\chi}_0 - \frac{TR}{c_1}\right)\exp\left(-\frac{c_1 j}{J_3}t\right) \le \max(TR/c_1, \dot{\chi}_0)$$

The transversal component F_η of reaction has the same value as in the previous case (Eq. 21), and the longitudinal one is:

$$F_\xi = -j\left(T\cos\theta - \frac{mR}{J_3}M_\eta\right) = -j\left(T\cos\theta + c_1\dot{\chi}\frac{mR}{J_3}\right) \tag{26}$$

If at the beginning the wheel is at rest (strictly speaking, initial speed $\dot{\chi}_0 \le TR/c_1$) then the reaction on the rectilinear motion $\theta = 0$ does not exceed T. Consequently, the slipping does not occur on rectilinear motion $\theta \equiv 0$ if $T \le fmg$. The FC-region for the maximal $\dot{\chi}$ is given by inequality

$$\left(j\cos\theta + 1 - j\right)^2 + \left(\sin\theta + \dot{\theta}\frac{J_3(1-j)}{c_1 j}\right)^2 \le T^{-2}f^2m^2g^2$$

It means, that if $T > fmg$ the slipping can occur for some large enough value of $\dot{\chi}$, but if $T < fmg$ there exists the initial values domains starting from where non-slipping condition can be ensured by Coulomb dry friction (fig. 2).

5 Distributed dry friction

Differential constraints (17) reduce the system (11)–(16) to the system (24)–(25): the order of the system decreases from 6th to 3rd. It allows getting qualitative analysis of the system. However, the system do not show the well-known shimmy-fenomenon when rectilinear motion loses its stability for some values of parameter. Below we use the distributed dry friction model to study the stability of rectilinear model.

5.1 Constructing of a model of friction

The wheel touches the visco-elastic plane $z = 0$ in point M. We denote its two principal radii of curvature in the contact point by A and B. We approximate the surface of the wheel by a paraboloid with $M\xi, M\eta$ being principal axes. So, the equation of the approximating surface of the wheel is:

$$\zeta(\xi,\eta) = \frac{1}{2}(A\xi^2 + B\eta^2), \text{ where } A = \frac{1}{2R},\ B = \frac{1}{2r}$$

Here r is a width of the wheel.

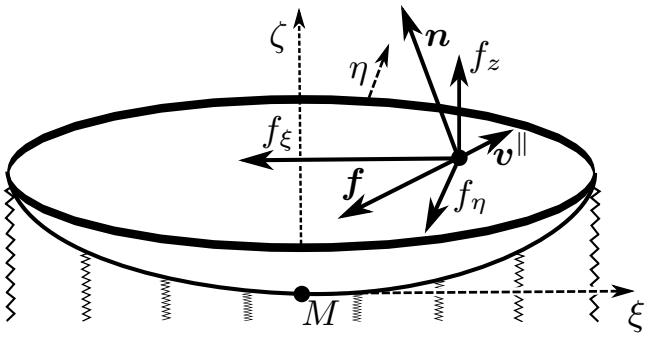

Fig. 3: Coordinate system and the densities of the forces acting in the contact patch.

We assume that the half-space $z \le 0$ is modelled by Winkler bedding: it consists of vertical springs that do not interact with each other. The springs' response on deformation is Kelvin-Voigt visco-elastic force $f_z d\Sigma$ with a density f_z in an infinitesimal area $d\Sigma = dx\,dy$:

$$f_z = \begin{cases} -kz - \nu\dot{z}, \text{ if } -kz - \nu\dot{z} > 0, \\ 0, \quad \text{if } -kz - \nu\dot{z} \le 0, \end{cases} \qquad k > 0,\ \nu > 0. \tag{27}$$

Here z is a vertical coordinate of the corresponding spring's top and $\dot{z}$ is its velocity. Assuming that each deformed spring touches the surface of the wheel, we express the vertical speed of the end of the spring with coordinates $\xi,\ \eta$ as

$$\dot{z} = v_z - \omega_\eta \xi + A\xi(-u_\xi + \omega_\zeta \eta - \omega_\eta \zeta(\xi,\eta)) + B\eta(-u_\eta - \omega_\zeta \xi)$$

where $u_\xi = v_\xi - \dot{\chi}R$, $u_\eta = v_\eta$ are the projections of the velocity of point M on $M\xi$, $M\eta$ axes, $\omega_\eta = \dot{\chi}$, $\omega_\zeta = \dot{\theta}$ (details can be found in [8]). Thus, the density of the vertical restoring force is

$$f_z = -k(z + \zeta(\xi,\eta)) - \nu\left[v_z - \omega_\eta \xi + A\xi(-v_\xi + \omega_\zeta \eta - \omega_\eta \zeta(\xi,\eta)) + B\eta(-v_\eta - \omega_\zeta \xi)\right]$$

The contact patch between the wheel and the plane is the set

$$\mathscr{J} = \{(\xi,\eta) : \zeta(\xi,\eta) < 0 \text{ and } f_z \ge 0\}.$$

We assume that each infinitesimal area of the contact patch acts on the wheel by the normal force $n\boldsymbol{n}$ and sliding dry Coulomb friction force $fn\frac{\boldsymbol{v}^{\parallel}}{v^{\parallel}}$, where

$$\boldsymbol{n} = \frac{\operatorname{grad}\Phi}{|\operatorname{grad}\Phi|} = \frac{-A\xi\boldsymbol{e}_\xi - B\eta\boldsymbol{e}_\eta + \boldsymbol{e}_\zeta}{\sqrt{1 + A^2\xi^2 + B^2\eta^2}}$$

is the inner normal vector of the paraboloid, and $\boldsymbol{v}^{\parallel}$ is the tangent component of each spring's velocity with respect to the wheel:

$$\boldsymbol{v}^{\parallel} = \dot{\xi}\boldsymbol{e}_\xi + \dot{\eta}\boldsymbol{e}_\eta + \dot{\zeta}\boldsymbol{e}_\zeta$$

where

$$\dot{\xi} = -u_\xi + \omega_\zeta \eta - \omega_\eta \zeta(\xi,\eta),\ \dot{\eta} = -u_\eta - \omega_\zeta \xi,\ \dot{\zeta} = A\xi\dot{\xi} + B\eta\dot{\eta}$$

Finally, the densities of horizontal forces are

$$f_\xi = n\left(-A\xi + f\dot{\xi}\frac{\sqrt{1 + A^2\xi^2 + B^2\eta^2}}{\sqrt{\dot{\xi}^2 + \dot{\eta}^2 + \dot{\zeta}^2}}\right), \quad f_\eta = n\left(-B\eta + f\dot{\eta}\frac{\sqrt{1 + A^2\xi^2 + B^2\eta^2}}{\sqrt{\dot{\xi}^2 + \dot{\eta}^2 + \dot{\zeta}^2}}\right).$$

where

$$n = f_z \left(1 + f\dot{\zeta} \frac{\sqrt{1+A^2\xi^2+B^2\eta^2}}{\sqrt{\dot{\xi}^2+\dot{\eta}^2+\dot{\zeta}^2}} \right)^{-1}.$$

We get the resultant force $\boldsymbol{F}$ and the torque $\boldsymbol{M}$ with respect to the point M by integrating over the contact patch $\mathscr{J}$:

$$F_z = \iint\limits_{\mathscr{J}} f_z \, d\Sigma, \quad F_\xi = \iint\limits_{\mathscr{J}} f_\xi \, d\Sigma, \quad F_\eta = \iint\limits_{\mathscr{J}} f_\eta \, d\Sigma$$

$$\boldsymbol{M} = \iint\limits_{\mathscr{J}} \left[\left(\xi \, \boldsymbol{e}_\xi + \eta \, \boldsymbol{e}_\eta + \zeta \, \boldsymbol{e}_\zeta \right) \times \left(f_\xi \, \boldsymbol{e}_\xi + f_\eta \, \boldsymbol{e}_\eta + f_z \boldsymbol{e}_z \right) \right] d\Sigma$$

5.2 Steady-state motions

Eqs. (11 - 16) allow one-parametric family of steady-state motions with the speed V of the wheel's center as a parameter:

$$z = z_0 = \text{const}, \; v_z = 0, \; v_\xi = V = \text{const}, \; v_\eta = 0, \; \theta = 0, \; R\dot{\chi} = v_\xi - u_\xi = V - u = \text{const} \tag{28}$$

Here $z \equiv z_0$ is a steady height of the wheel center and $u_\xi \equiv u$ is a steady slipping speed. Indeed, for this motions we have the following density of vertical forces

$$f_z = -k(z + \zeta(\xi,\eta)) - \nu \left[(u-V)\xi + A\xi(-VR + (u-V)\zeta(\xi,\eta)) \right] / R$$

Calculating horizontal densities we get

$$\dot{\xi} = -u + (u-V)\zeta(\xi,\eta)/R, \; \dot{\eta} = 0, \; \dot{\zeta} = A\xi\dot{\xi}$$

and

$$n = f_z \left(1 + fA\xi \operatorname{sign}\dot{\xi} \frac{\sqrt{1+A^2\xi^2+B^2\eta^2}}{\sqrt{1+A^2\xi^2}} \right)^{-1},$$

$$f_\xi = n \left(-A\xi + f \operatorname{sign}\dot{\xi} \frac{\sqrt{1+A^2\xi^2+B^2\eta^2}}{\sqrt{1+A^2\xi^2}} \right), \quad f_\eta = -B\eta n.$$

Since f_z, n, f_ξ depends only on squared variable η, the contact patch $\mathscr{J}$ is symmetrical with respect to ξ-axis and the components F_η, M_z vanish. Substituting the steady-state motions into Eqs. (11 - 16), we get only three equations that are not trivially fulfilled:

$$0 = F_z - mg \tag{29}$$

$$0 = F_\xi + T \tag{30}$$

$$0 = -F_\xi R + M_\eta \tag{31}$$

For any desired speed V we can find the parameters z_0 and u from Eqs. (29, 31), and Eq. (30) gives the value for the driving force T. Notice that the solution does not depend on the parameter b. The solution is found numerically by means of GNU Scientific Library methods [10] and is shown on Fig. 4. The parameters of the system in the numerical simulations here and further are:

$$m = 5, \; J_1 = 0.5, \; J_3 = 1, \; R = 1, \; r = 0.16, \; f = 0.2, \; k = 10, \; \nu = 1, \; g = 9.8$$

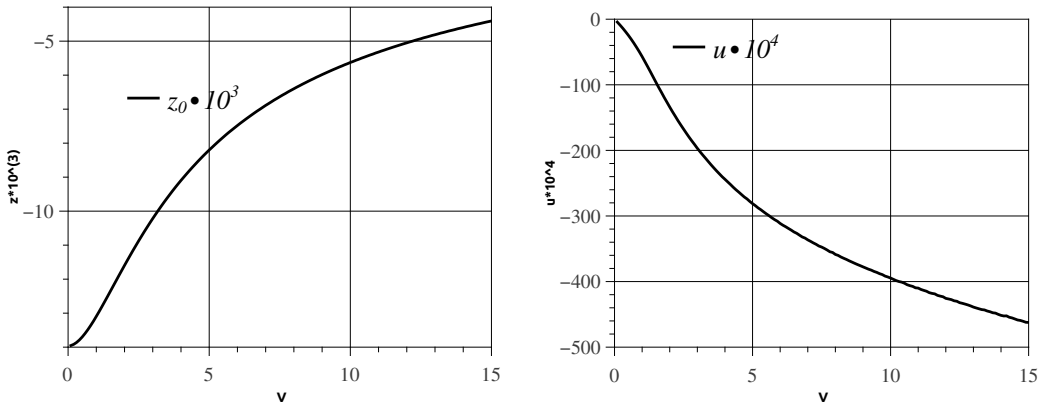

Fig. 4: Steady-state height z_0 of the wheel center and slipping speed u versus the center's speed V.

5.3 Linearization in the vicinity of steady-state motions

We will study the stability of steady-state motions through linear analysis. We introduce the deviations of variables in the vicinity of steady-state solution:

$$z = z_0 + \delta z,\ \dot{z} = \delta v_z,\ v_\xi = V + \delta v_\xi,\ v_\eta = \delta v_\eta,\ \theta = \delta\theta,\ \dot{\theta} = \delta\omega_\zeta,\ \dot{\chi} = (V-u)/R + \delta\omega_\eta$$

Linearizing Eqs. (11–16), we get:

$$\begin{aligned}
(\delta z)^{\cdot} &= \delta v_z \\
m(\delta v_z)^{\cdot} &= \delta F_z \\
m(\delta v_\xi)^{\cdot} &= \delta F_\xi \\
J_3(\delta\omega_\eta)^{\cdot} &= -R\,\delta F_\xi + \delta M_\eta \\
m(v_\eta)^{\cdot} &= \delta F_\eta - T\,\delta\theta - mV\,\delta\omega_\zeta \\
J_1(\delta\omega_\zeta)^{\cdot} &= \delta M_z - bT\,\delta\theta \\
(\delta\theta)^{\cdot} &= \delta\omega_\zeta
\end{aligned} \tag{32}$$

Here

$$\delta F_\cdot = \sum \frac{\partial F_\cdot}{\partial x}\bigg|_{\text{Eq. (28)}} \delta x, \quad \delta M_\cdot = \sum \frac{\partial M_\cdot}{\partial x}\bigg|_{\text{Eq. (28)}} \delta x, \qquad x = \{z, v_z, v_\xi, \omega_\eta, v_\eta, \omega_\zeta, \theta\}$$

are variations of the forces and torques in the vicinity of steady motion, the derivatives are calculated on the steady motions Eq. (28) (further we will skip this notation in formulas).

Friction forces possesses the following properties:

1. The variable θ is a cyclic variable: the shift on this variable is equivalent to the rotation of inertial coordinate frame about the vertical axis Oz. So the forces and torques do not depend on theta

$$\frac{\partial F_\cdot}{\partial\theta} = 0,\ \frac{\partial M_\cdot}{\partial\theta} = 0$$

2. The "transversal" components F_η, M_z vanishes for $v_\eta = 0$, $\omega_z = 0$ and arbitrary values of z, v_z, v_ξ, ω_η, so we have

$$\frac{\partial F_\eta}{\partial z} = 0,\ \frac{\partial F_\eta}{\partial v_z} = 0,\ \frac{\partial F_\eta}{\partial v_\xi} = 0,\ \frac{\partial F_\eta}{\partial\omega_\eta} = 0$$

$$\frac{\partial M_z}{\partial z} = 0,\ \frac{\partial M_z}{\partial v_z} = 0,\ \frac{\partial M_z}{\partial v_\xi} = 0,\ \frac{\partial M_z}{\partial\omega_\eta} = 0$$

3. Vertical and "longitudinal" components F_z, F_ξ, M_η are even functions of each v_η, ω_ζ, so

$$\frac{\partial F_z}{\partial v_\eta} = 0,\ \frac{\partial F_z}{\partial \omega_\zeta} = 0, \quad \frac{\partial F_\xi}{\partial v_\eta} = 0,\ \frac{\partial F_\xi}{\partial \omega_\zeta} = 0, \quad \frac{\partial M_\eta}{\partial v_\eta} = 0,\ \frac{\partial M_\eta}{\partial \omega_\zeta} = 0$$

These properties give that the matrix of the system Eq. (32) has the structure

$$(\delta x)^{\cdot} = \boldsymbol{A}\delta x, \quad x = \{z, v_z, v_\xi, \omega_\eta, v_\eta, \omega_\zeta, \theta\} \tag{33}$$

$$\boldsymbol{A} = \begin{pmatrix} 0 & 1 & 0 & 0 & 0 & 0 & 0 \\ \frac{1}{m}\frac{\partial F_z}{\partial z} & \frac{1}{m}\frac{\partial F_z}{\partial v_z} & \frac{1}{m}\frac{\partial F_z}{\partial v_\xi} & \frac{1}{m}\frac{\partial F_z}{\partial \omega_\eta} & 0 & 0 & 0 \\ \frac{1}{m}\frac{\partial F_\xi}{\partial z} & \frac{1}{m}\frac{\partial F_\xi}{\partial v_z} & \frac{1}{m}\frac{\partial F_\xi}{\partial v_\xi} & \frac{1}{m}\frac{\partial F_\xi}{\partial \omega_\eta} & 0 & 0 & 0 \\ \frac{1}{J_3}\frac{\partial(-RF_\xi+M_\eta)}{\partial z} & \frac{1}{J_3}\frac{\partial(-RF_\xi+M_\eta)}{\partial v_z} & \frac{1}{J_3}\frac{\partial(-RF_\xi+M_\eta)}{\partial v_\xi} & \frac{1}{J_3}\frac{\partial(-RF_\xi+M_\eta)}{\partial \omega_\eta} & 0 & 0 & 0 \\ 0 & 0 & 0 & 0 & \frac{1}{m}\frac{\partial F_\eta}{\partial v_\eta} & \frac{1}{m}\frac{\partial F_\eta}{\partial \omega_\zeta} - V & -\frac{T}{m} \\ 0 & 0 & 0 & 0 & \frac{1}{J_1}\frac{\partial M_z}{\partial v_\eta} & \frac{1}{J_1}\frac{\partial M_z}{\partial \omega_\zeta} & -\frac{bT}{J_1} \\ 0 & 0 & 0 & 0 & 0 & 1 & 0 \end{pmatrix} \tag{34}$$

The matrix $\boldsymbol{A}$ is block-diagonal and is partitioned into two submatrix of sizes 4×4 ("longitudinal") and 3×3 ("transversal"). As each steady-state solution does not depend on the offset of the fork b, then all the components of $\boldsymbol{A}$ except for explicitly shown do not depend on this parameter.

5.4 The stability of transversal subsystem

Since shimmy phenomenon occurs when the variable θ increases, we will study the transversal subsystem of Eq. 33. It reads:

$$\frac{d}{dt}\begin{pmatrix}\delta v_\eta \\ \delta\omega_\zeta \\ \delta\theta\end{pmatrix} = \begin{pmatrix} a_{11} & a_{12} & -T/m \\ a_{21} & a_{22} & -bT/J_1 \\ 0 & 1 & 0 \end{pmatrix}\begin{pmatrix}\delta v_\eta \\ \delta\omega_\zeta \\ \delta\theta\end{pmatrix} \tag{35}$$

where

$$a_{11} = \frac{1}{m}\frac{\partial F_\eta}{\partial v_\eta},\ a_{12} = \frac{1}{m}\frac{\partial F_\eta}{\partial \omega_\zeta} - V,\ a_{21} = \frac{1}{J_1}\frac{\partial M_z}{\partial v_\eta},\ a_{22} = \frac{1}{J_1}\frac{\partial M_z}{\partial \omega_\zeta}$$

The characteristic polynom is

$$\lambda^3 - (a_{11}+a_{22})\lambda^2 + \left(a_{11}a_{22} - a_{21}a_{12} + \frac{bT}{J_1}\right)\lambda - \frac{a_{11}bT}{J_1} + \frac{a_{21}T}{m} = 0$$

The Routh-Hurvitz stability criterion for this system has the form:

$$a_{11} + a_{22} < 0$$

$$\frac{a_{21}T}{m} - \frac{a_{11}bT}{J_1} > 0$$

$$\left(a_{11}a_{22} - a_{21}a_{12} + \frac{bT}{J_1}\right)(a_{11}+a_{22}) - \frac{a_{11}bT}{J_1} + \frac{a_{21}T}{m} < 0$$

Collecting terms and substituting the notations, we get

$$\frac{1}{m}\frac{\partial F_\eta}{\partial v_\eta} + \frac{1}{J_1}\frac{\partial M_z}{\partial \Omega} < 0$$

$$b > \frac{\partial M_z}{\partial v_\eta} \Big/ \frac{\partial F_\eta}{\partial v_\eta} \tag{36}$$

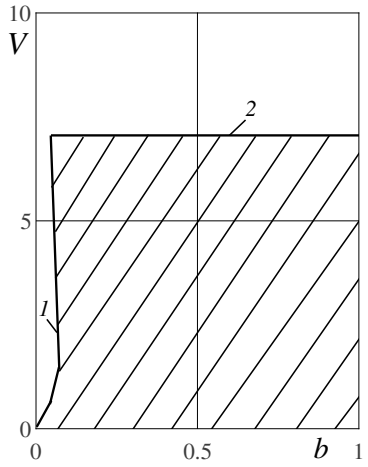

Fig. 5: Stability region: b is the offset of the fork, V is the steady-state speed of the wheel's center.

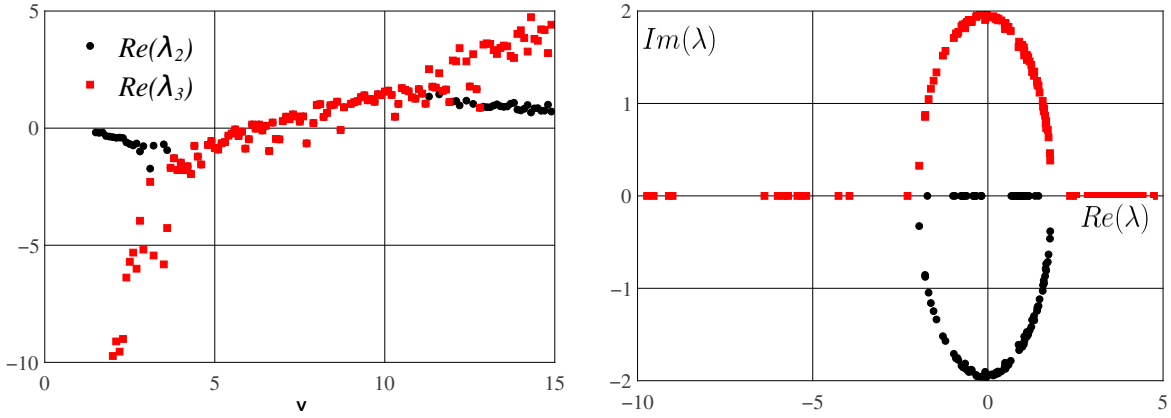

Fig. 6: Left panel: Real parts versus V of "transversal" subsystem's eigenvalues; right panel: Imagine parts versus real parts

$$\frac{bT}{J_1}a_{22} < -(a_{11}a_{22} - a_{21}a_{12})(a_{11} + a_{22}) - \frac{a_{21}T}{m}$$

We got numerically that a_{11} and a_{22} are negative for the considered values of the parameters, so the first inequality holds and the third one has the form:

$$b > -\frac{J_1(a_{11}a_{22} - a_{21}a_{12})(a_{11} + a_{22})}{a_{22}T} - \frac{J_1 a_{21}}{a_{22}m} \tag{37}$$

The derivatives were calculated numerically in GNU Scientific Library basing on discrete calculation of the forces ant torques. The region of stability is shaded on Fig. 5. The curve 1 corresponds to Ineq. 36, the curve 2, which has small positive slope, corresponds to Ineq. 37. It follows that the steady-state motion is stable for $b > b_0(V) \approx 6 \cdot 10^{-2}$ and $0 < V < V_0(b) \approx 7$.

We calculated the eigenvalues of the transversal system Eq. eq:transversal for $b = 0.9$ for $V \in [0,\ 15]$. One of them λ_1 always has negative real part. The real parts of $\lambda_{2,3}$ are shown on the left panel of Fig. 6. They are real and have negative real parts till $V \approx 3.7$, for $V \in [3.7,\ 12.5]$ eigenvalues $\lambda_{2,3}$ are complex and their real parts are positive for $V > 7$. Finally, λ_1, λ_2 are real and have positive real parts for $V > 12.5$. On the right panel of Fig. 6, the imaginary values of λ_1, λ_2 are plotted versus their real parts. Thus, the Poincaré-Andronov-Hopf bifurcation occurs at $V \approx 7$.

We numerically simulate the acceleration of the wheel that starts from the rest with small initial angle θ. We take

$$T = 5,\ \theta(0) = 0.1,\ \dot{\chi} = 0$$

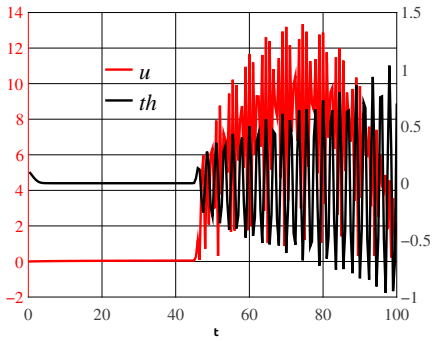

Fig. 7: Shimmy occurs during the acceleration of the wheel.

The dependence of the course angle θ through time is shown on Fig. 7 by black line, red line shows the value of slipping $u = \sqrt{u_\xi^2 + u_\eta^2}$. While the speed is small, θ fastly decreases to zero, but after approximately 45 time-units the oscillation begins and grows significantly up to a certain finite amplitude.

6 Conclusions

Three models of ground-wheel interaction were considered. In first two cases the reaction forces are calculated from the equations of motions and imposed non-holonomic constraints of non-slipping. The steady rectilinear motion with the wheel center behind the fork is stable. Under the action of the constant driving force in any vicinity of the stable steady solution the wheel accelerates till the moment when the wheel slips. After that, the stability results can not be applied to the system. Rolling and spinning friction makes the steady solution asymptotically stable and bound the maximal speed of the wheel. For small values of driving force (they depend on the coefficient of dry friction) there exists the vicinity of the steady motion without sliding in it, and, consequently, no shimmy. For the distributed dry friction, the steady-state rectilinear motions are found and their stability is studied. It is shown that the Poincaré-Andronov-Hopf bifurcation occur. The stability region is plotted. In addition, the numerical simulation of the wheel starting from rest under the constant force is performed: shimmy oscillation occurs after the wheel accelerates enough.

Acknowledgements

The work is supported by Russian Foundation for Basic Research (project 16-01-00338).

References

[1] B. Feeny, A. Guran, N. Hinrichs, and K. Popp, “A historical review on dry friction and stick-slip phenomena,” *Applied Mechanics Reviews*, vol. 51, no. 5, pp. 321–341, 1998.

[2] M. Keldysh, “Shimmi perednego kolesa trehkolesnogo shassi,” *Trudy CAGI*, vol. 1, no. 564, pp. 1–37, 1945. (Russian).

[3] Y. I. Nejmark and N. Fufaev, *Dinamika negolonomnyh sistem*. Moscow, Russia: Nauka, 1 ed., 1967.

[4] O. A. Bauchau and J. Rodriguez, “Simulation of wheels in nonlinear, flexible multibody systems,” *Multibody System Dynamics*, vol. 7, no. 4, p. 407438, 2002.

[5] G. Stépán, “Chaotic motion of wheels,” *Vehicle System Dynamics*, vol. 20, no. 6, pp. 341–351, 1991.

[6] D. Takács, G. Stépán, and S. Hogan, “Isolated large amplitude periodic motions of towed rigid wheels,” *Nonlinear Dynamics*, vol. 52, no. 1, pp. 27–34, 2008.

[7] V. Zhuravlev and D. Klimov, “Theory of the shimmy phenomenon,” *Mechanics of Solids*, vol. 45, no. 3, pp. 324–330.

[8] A. A. Zobova, "Dry friction distributed over a contact patch between a rigid body and a visco-elastic plane," in *Proceedings of the EUROMECH Colloquium 578. Rolling Contact Mechanics for Multibody System Dynamics*, pp. 1–18, Institute of Mechanical Engineering (IDMEC), Portugal Funchal, Madeira, Portugal, 2017.

[9] A. A. Zobova, "Application of laconic forms of the equations of motion in the dynamics of nonholonomic mobile robots," *Rus. J. Nonlin. Dyn.*, vol. 7, no. 4, pp. 771–783, 2011. (Russian).

[10] `https://www.gnu.org/software/gsl/`.